Electrochemical study of nitrostilbene derivatives: nitro group as a probe of the push–pull effect

S. Bollo [a], E. Soto-Bustamante [b], L.J. Núñez-Vergara [a], J.A. Squella [a,*]

[a] *Department of Organic Chemistry, Bioelectrochemistry Laboratory, Chemical and Pharmaceutical Sciences Faculty, University of Chile, PO Box 233, Santigo 1, Chile*

[b] *Liquid Crystal Laboratory, Chemical and Pharmaceutical Sciences Faculty, University of Chile, PO Box 233, Santigo 1, Chile*

Abstract

This paper reports electrochemical (tast polarography, differential pulse polarography, cyclic voltammetry) and spectroscopic investigations covering a series of stilbene derivatives having either one or two electron-donating groups (alkoxy, hydroxy, phenolate at pH > 9) located at one end of the molecules. The groups interact, through a conjugated system of π electrons, with an electron-withdrawing group (nitro group) at the opposite end of the molecule. The push–pull effect on the molecule is obtained by the presence of the extended unsaturated π electron system combined with a polar substituent with opposite electrical effects suitably attached to the conjugated systems. This arrangement gives relevant electro-optics characteristics to the molecules. The polar substituents are electroactive and, by comparison of the potential peaks of the compounds, it is possible to estimate the intramolecular electronic interactions within the molecule. Specifically, in this case, change in the potential peak of the nitro group allows conclusions about the push–pull effect in the system to be reached.

Keywords: Nitrostilbene derivatives; Push–pull effect; Electroreduction

1. Introduction

The increase of the passage of information nowadays requires new mechanisms for signal translation. The way to accomplish this is by using light instead of electrons for information processing. Therefore it is necessary to design new materials with non-linear optic (NLO) properties, especially second order non-linearity [1], useful e.g. in frequency conversion. For this task, a macroscopic polar order is required that, usually, is rather poor in organic materials. Different strategies have been tested looking for a preferential orientation of polar molecules. Guest–host systems where dyes are dissolved in a polar matrix, co- and homopolymers possessing liquid crystalline properties with pendant chromophores and so on are some examples already investigated [2–4].

To investigate the polar order, the hyperpolarizability needs to be calculated by different methods like solvatochromy [5] or the displacement of the absorption band in solvents of different dielectric constant. A direct method is the second harmonic generation (SHG) experiment [6] that gives directly the component of the piezoelectric tensor responsible for the hyperpolarizability. On the other hand, electrochemical methods permit information to be obtained about the energy required in a redox process of organic molecules that have electroactive groups. Therefore we are interested in using an electrochemical route to investigate the polar order in organic compounds possessing electroactive centers.

The synthesis of liquid crystalline molecules with large hyperpolarizability [7] and monomers [8] was carried out with organic compounds having extended unsaturated π electron systems. The strategy was to include groups with opposite electron affinities, like nitro and alkoxy groups attached to a conjugated aromatic core. Such a so-called push–pull system results in molecules with large ground-state dipole moments.

E-mail address: asquella@ll.ciq.uchile.cl (J.A. Squella).

The subject of this work is to use the electroactive nitro group as a probe to investigate the polar order in a series of organic dyes containing an azomethine group and a nitrostilbene or a nitroazobenzene moiety. In a previous work we have used the nitro group as a probe to investigate steric and electronic effects in a series of β-nitrostyrene derivatives [9]. Despite the fact that several papers on the electrochemical study of aromatic, heterocyclic and aliphatic nitro compounds have been published [10–15], the electrochemistry of organic dyes containing nitrostilbene is an unexplored field of research. Furthermore this type of compound attracted our attention because it represents a very special type of molecule where long-distance transmission of electronic effects through the molecule can be observed. Consequently the electrochemical approach can be a useful tool in order to investigate the behavior of push–pull systems in highly conjugated molecules.

In a further stage of this research, the information related to the conjugation of the system can be compared with its NLO-properties looking for a new method to estimate the dipolar arrangement in conjugated organic systems.

2. Experimental

2.1. Reagents and solutions

All the compounds were synthesized and characterized following a procedure reported previously [8]. All other reagents employed were of analytical grade.

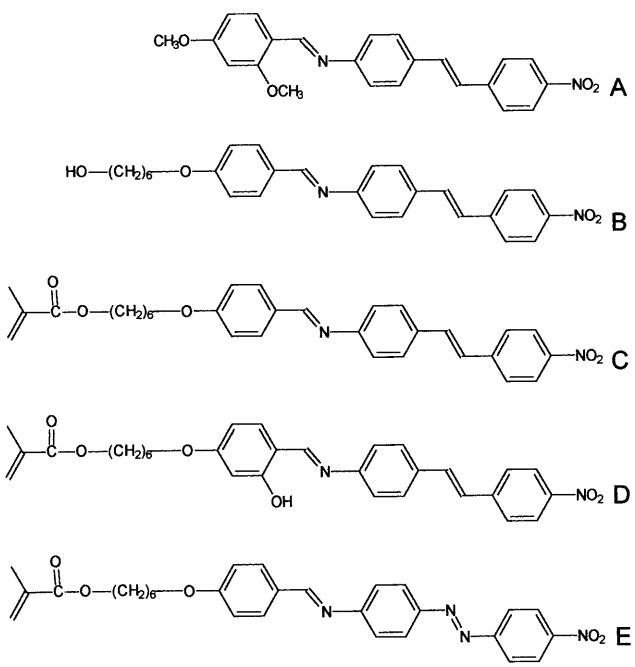

Fig. 1. Molecular structure of nitrostilbene derivatives.

Stock solutions of each compound were prepared at a constant concentration of 0.025 M in DMF. The polarographic working solutions were prepared by diluting the stock solution to obtain a final concentration of 0.1 mM. Solutions for cyclic voltammetry were prepared by weighing an adequate quantity of each compound in order to obtain a final concentration of 1 mM.

Due to the poor solubility of the molecules in aqueous solutions, experiments were made in mixed (DMF + buffer citrate: 60/40) and aprotic (100% DMF) media.

pH measurements were corrected according to the following equation [16]: $pH^* - B = \log U^{\circ}_{H}$ where pH* equals $-\log a_H$ in the mixed solvent, B is the pH meter reading and the term $\log U^{\circ}_{H}$ is the correction factor for the glass electrode, which was calculated from the different mixtures of DMF and aqueous solvent, according to a procedure reported previously [17].

2.2. Apparatus

Electrochemical experiments, differential pulse polarography (DPP), tast polarography and cyclic voltammetry (CV) were performed with a totally automated BAS CV-50W voltammetric analyzer. A 10 ml thermostated measuring cell, with three electrodes, dropping mercury electrode (DPP and tast polarography) and hanging mercury electrode (CV) as a working electrode, a platinum wire counter electrode, and a saturated calomel reference electrode, were used for the measurements.

Spectrophotometric measurements were carried out with an UV–Vis spectrophotometer ATI Unicam model UV3, using a 1 cm quartz cell and equipped with a 486 computer with vision acquisition and treatment program.

3. Results and discussion

All compounds were electrochemically reduced at DME in mixed media (DMF + citrate buffer: 60/40). According to the molecular structures (Fig. 1), the electroreducible groups in molecules **A**–**D** are the nitro and azomethine moieties, and in molecule **E** also the azo group. Fig. 2 shows the differential pulse (DPP) and tast polarograms (TP) for compounds **A**–**D**. The signals correspond to the electroreduction of the nitro group (peak I and wave I) and azomethine group (peak II and wave II). The peak II is poorly resolved by the DPP technique and is totally un-resolved by TP. The polarograms of compound **E** are

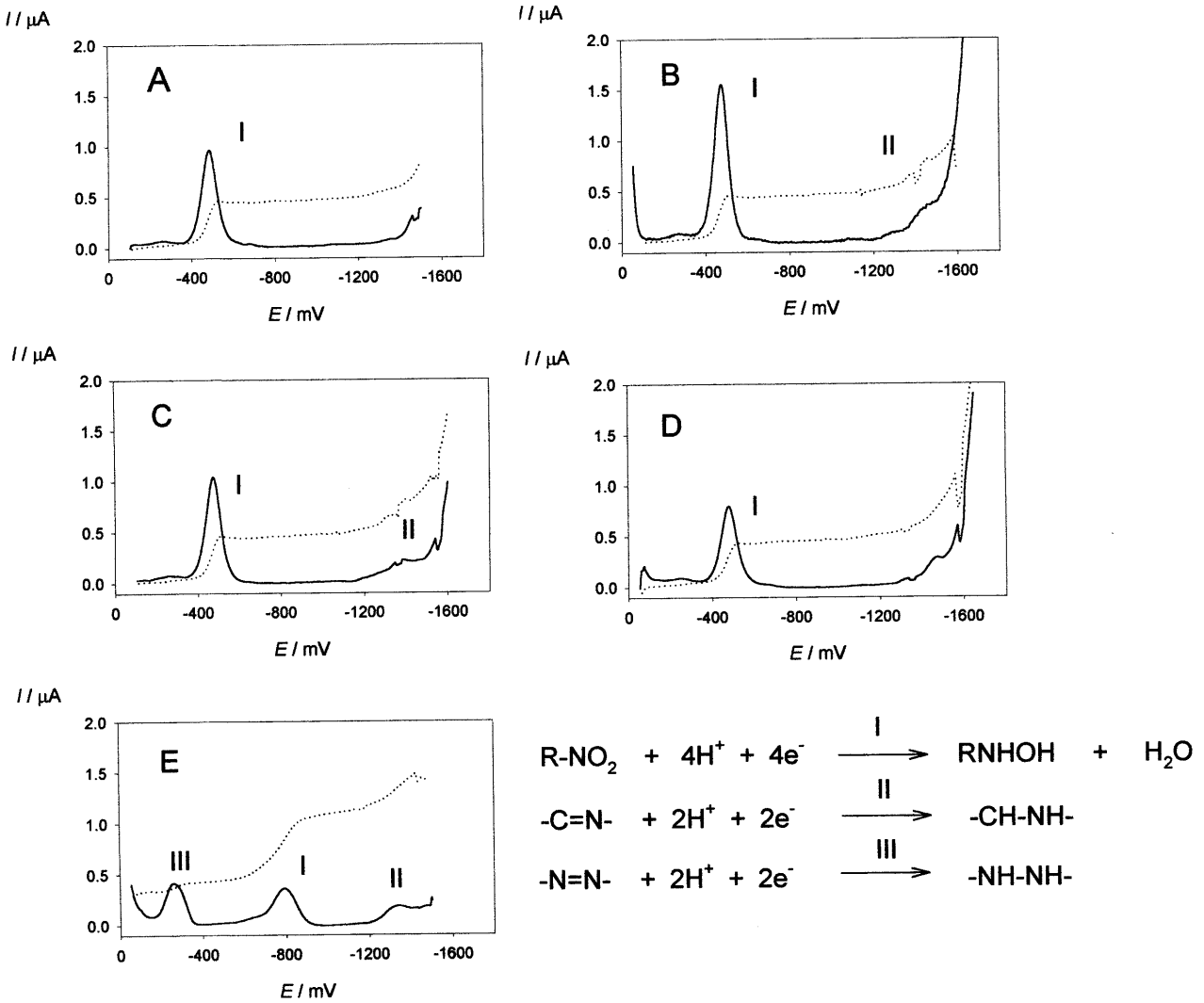

Fig. 2. Differential pulse (solid line) and tast (dashed line) polarograms of several nitrostilbene derivatives at pH 7 in mixed media, DMF + citrate buffer: 60/40. Molecules **A** to **D** containing two electroreducible groups (nitro and azomethine groups) and molecule **E** containing three electroreducible groups (nitro, azomethine and azo groups).

rather different showing a new peak III or wave III, assigned to the reduction of the azo group.

The reduction of these groups is strongly pH-dependent. Both the limiting current and potential peak change with pH. In Figs. 3(A) and 4(A), the peak potential versus pH plots for compounds **A** and **E** are shown. For compound **A**, the reduction of both the nitro and azomethine group varies towards more negative values as the pH increases until approximately pH 8–9. At pH < 4 a polarographic maximum in the wave I appears. This effect probably produces a distortion of the limiting current. In alkaline media, pH ≥ 9, peak I is totally pH-independent and a new peak appears (peak I′). It is located at more negative potential due to a splitting of the nitro reduction signal (peak I). On the other hand, at pH 4 a change in the slope of the linear relationship for the nitro reduction and a break between pH 5–6 in the azomethine reduction is observed. Probably this break indicates changes in the mechanism for the azomethine group reduction process, due to protonation–deprotonation equilibrium in the molecule. Compounds **B**, **C** and **D** follow a similar pH dependence on E_p as discussed above for compound **A** (Fig. 3).

In Fig. 3(B) the evolution of the limiting current with pH for compound **A** is observed. The limiting current due to nitro reduction was pH-independent until pH 7, showing diffusion-controlled behavior. Above pH 8, the limiting current decreased when pH increased. Concomitant with this decrease, a new wave is observed. The limiting current of this new wave increased when pH increased. The sum of the limiting current for both waves (peak I and I′) is comparable to the initial limiting current, showing that this effect is due to a

splitting of the initial wave. This behavior is in accordance with the following well-known mechanism for the reduction of nitroaromatic compounds [10,11]:

At $pH < 8$

$$ArNO_2 + 4e^- + 4H^+ \rightarrow ArNHOH + H_2O \quad (1)$$

At $pH > 8$

$$ArNO_2 + e^- \Leftrightarrow ArNO_2^{\bullet -} \quad (2)$$

$$ArNO_2^{\bullet -} + 3e^- + 4H^+ \rightarrow ArNHOH + H_2O \quad (3)$$

In the case of compounds **B**, **C** and **D**, the limiting current behaves similarly to that for compound **A**. Table 1 summarizes the potential peaks of the nitro group for all compounds at different pH values. Compound **A** is more difficult to reduce than compounds **B** and **C** by about 75 mV at pH 3 and 18 mV at pH 6. This can be explained due to the presence of two electron-donating substituents in **A**. The effect of a second alkoxy group becomes less important as the pH increases and is not shown at pH 9 and higher. This probably reflects the fact that the protonated nitro group is more electron withdrawing than the non-protonated. Also, the hydroxy group in **D** seems to have

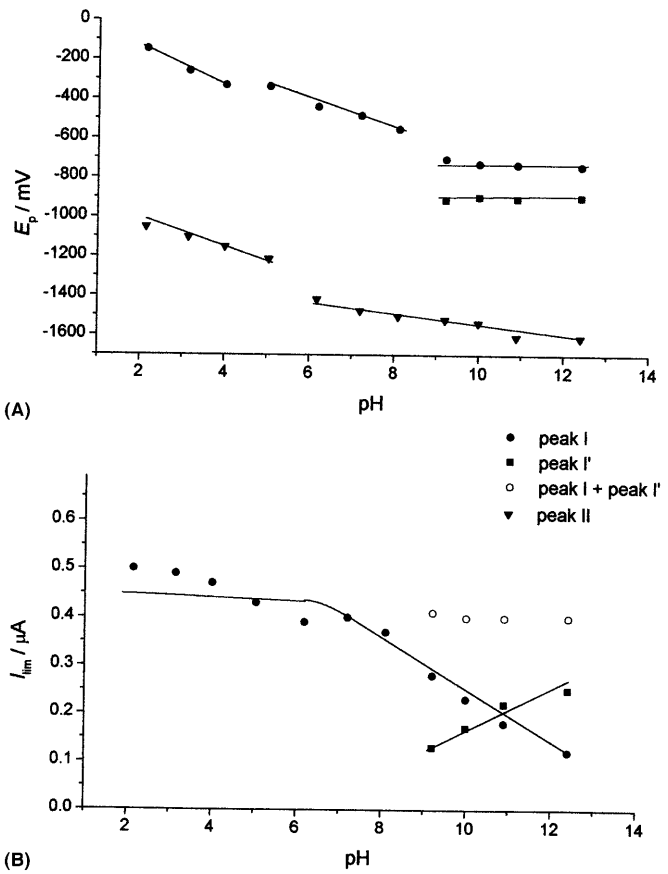

Fig. 3. Potential peak and limiting current dependence on pH for a 0.1 mM solution of compound **A** in DMF + citrate buffer: 60/40.

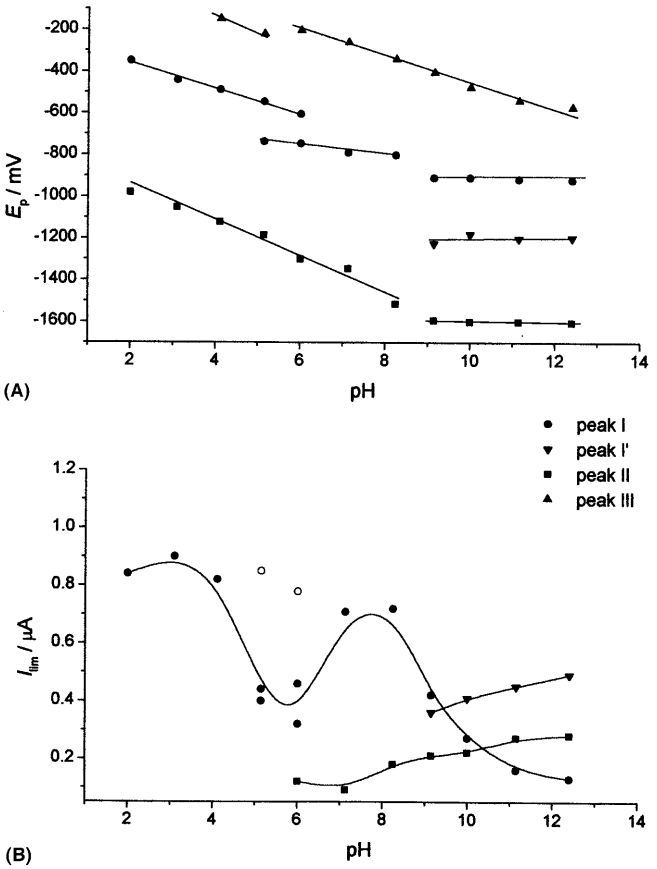

Fig. 4. Potential peak and limiting current dependence on pH for a 0.1 mM solution of compound **E** in DMF + citrate buffer: 60/40.

Table 1
Peak potentials of the nitro group in several nitrostilbenes (compounds **A**–**D**) at different pH values and the apparent pK values determined spectrophotometrically [a]

	E_p/mV				pK'_a
	pH 3	pH 6	pH 9	pH 12	UV–Vis
A	−260	−440	−704	−740	3.59
B	−186	−422	[b]	[b]	3.66
C	−180	−416	−704	−740	3.64
D	−182	−422	−702	−758	3.59–9.68
E′	−438	−654	−910	−922	

[a] Compound **E′** corresponds to the hydrazo derivative of compound **E**.
[b] Compound **B** precipitates out.

no effect at pH 3 and 9. A hydroxy group is only slightly less electron-donating than a methoxy group since its donating effect is probably cancelled by intramolecular hydrogen bonding to the nitrogen of the imino group. At pH 12, the hydroxy group exists as phenolate, which is a very strong electron-donating substituent, thus resulting in a more difficult reduction process for **D**, shifted by 18 mV when compared with **A** and **C**.

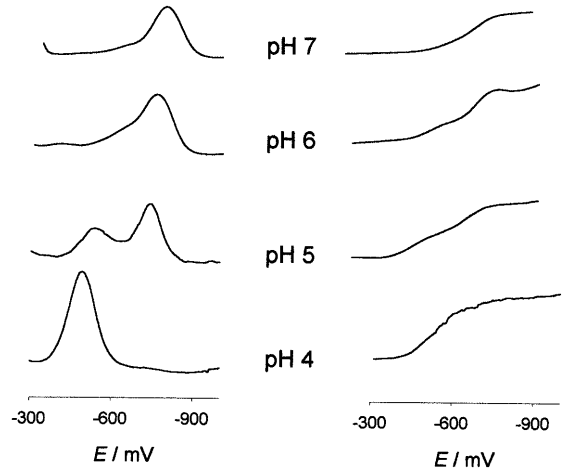

Fig. 5. Differential pulse and tast polarograms showing the protonation–deprotonation equilibrium of the nitro group in compound **E** at acidic pH values.

On the other hand, for compound **E** the behavior is rather different. In this case we have an electroactive azo group in the molecule instead of a carbon–carbon double bond. Consequently, between pH 2 and 8, it is possible to observe three main signals that belong to the nitro(I), azomethine(II) and azo group (III), respectively. In this pH zone, all peaks or waves are pH-dependent (Fig. 4(A)). At pH above 8, in a similar way as observed in compounds **A**–**D**, there is a splitting of the peak due to the nitro group. In this pH region the potential peaks I, I′ and II are pH independent. The potential of peak III decreases at pH higher than 8. Fig. 4(A) shows the variation of the peak potential with pH for compound **E**. This plot has some important differences with respect to the plot of Fig. 3(A) for compounds lacking the azo group. First, the peak potential reported for compound **E** corresponds to the reduction process of the hydrazo derivative (ArNH–NH–$C_6H_4NO_2$, see Table 1 compound **E**′) that clearly occurs at more negative potential values. This fact means that the reduction of the nitro group is more difficult due to a higher electron density enhanced by the hydrazo group (a fairly good electron donor) when compared with the other compounds without the nitrogen–nitrogen double bond. Second, for compound **E** a break between pH 5–6 in the azomethine group reduction for the E_p versus pH dependence (see Fig. 4(A)) is

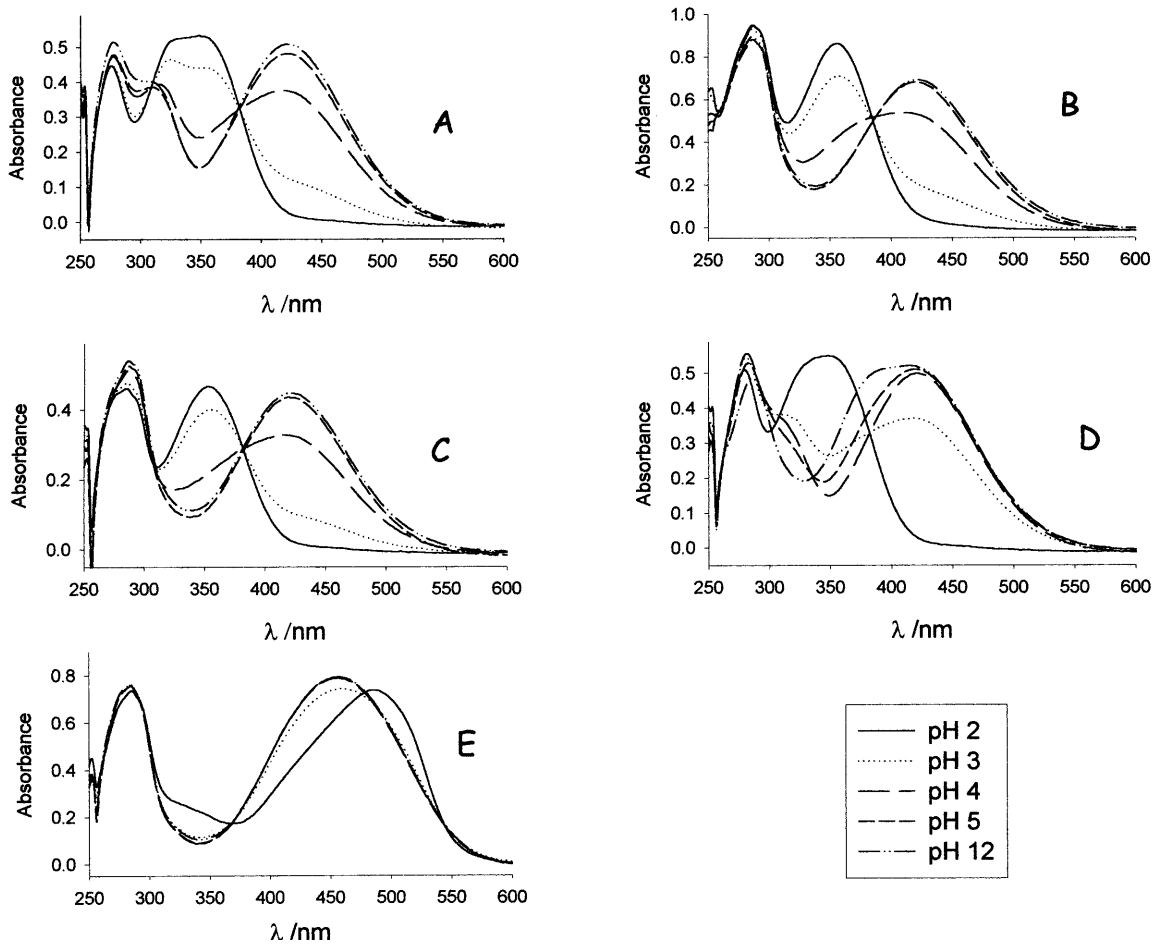

Fig. 6. UV–Vis spectra of several nitrostilbene derivatives at differents pH values between 2 and 12.

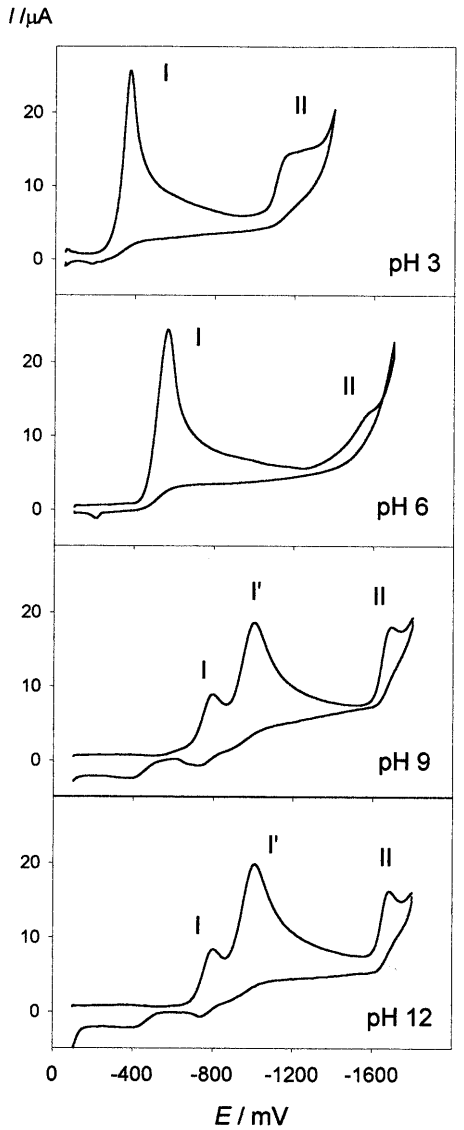

Fig. 7. Cyclic voltammograms of 1 mM of compound **A** in mixed media, DMF + citrate buffer: 60/40 at different pH values. Sweep rate 1 V s^{-1}. Note that cathodic currents are taken as positive.

not observed. Therefore, in compound **E** it is not possible to postulate protonation–deprotonation equilibrium for the azomethine group. Third the presence of two signals between pH 4 and 7 in the curve corresponding to the E_p evolution for the nitro reduction with pH (Figs. 4(A) and 5) was observed. These two signals correspond to a change in the electroactive species. This is clearly seen in Fig. 5 where one peak decreases in intensity at $E = -400$ mV while the other appears at $E = -750$mV as the pH increases. Then, at more acidic pH values (between 2 and 4) the electroreducible species is protonated and at higher pH values, the electroreducible specie is non-protonated. As expected, the protonated species is more easily reducible than the non-protonated. This behavior can be related to the protonation–deprotonation equilibrium for the nitro group due to the higher electron density discussed above.

In order to obtain additional evidence of the pH dependence in the protonation–deprotonation process of the molecule, we also evaluated the pH effect from the UV–Vis spectra. In Fig. 6 the spectrum of each compound at different pH values is observed. As observed by polarography, the UV–Vis behavior for compound **E** is rather different when compared with compounds **A**–**D**. In these compounds an absorption band at approximately 350 nm at acidic pH, that is absent in compound **E**, was observed. This band is strongly pH dependent, decreasing in intensity when the pH increases, then disappearing totally at pH values above 5. Associated with this decrease, a new absorption band appears in the visible zone at approximately 425 nm. We have used both the decrease of the band at 325 nm and the increase of the band at 425 nm to obtain the dissociation constants for the compounds expressed as pK'_a (see Table 1). These pK'_a values represent the protonation–deprotonation of the azomethine moiety. This assumption is in accordance with the break in the E_p versus pH curve between pH 5–6 in the azomethine group reduction already discussed. The curve for pH 12 in Fig. 6 for compounds **A**–**C** was completely reproducible for pH between 6 and 11. In compound **D** a second value of pK'_a was determined associated with the hydroxy substituent in the third ring that also indicates a protonation–deprotonation process and that the dissociation state of the molecule affects the electroreduction mechanism, changing the slope and producing breaks in the E_p versus pH plot.

This result is evidence of a push–pull effect favored in compound **E** due to the azo group. In fact the presence of the azo group in this molecule produces a pull effect on the azomethine group, diminishing the electron density and making its protonation more difficult. Consequently a pK'_a was not observed for this molecule. Furthermore, the protonation of the azomethine group at acidic pH values in compounds **A**–**D** hinders the conjugation producing an absorption band at approximately 350 nm. When the azomethine group is non-protonated the conjugation is increased producing an absorption band at approximately 425 nm. In compound **E** the azomethine group is always non-protonated and consequently the conjugation is always present as is shown by the band at approximately 450 nm. In conclusion there is spectroscopic evidence in accordance with an enhancement of the push–pull effect in molecule **E** due to the presence of the azobenzene group.

For a better understanding of the electrochemical behavior of the compounds, we used the cyclic voltammetry technique. In mixed media, the cyclic voltammographic behavior on mercury electrode is equivalent to that observed from polarography experiments: compounds **A**–**D** show very similar cyclic voltammograms and compound **E** shows a rather different response. Fig. 7 shows the cyclic voltammograms of compound **A**. The peaks correspond to the electroreduction of the nitro group (peak I) to generate the hydroxylamine derivative and the imino group (peak II) in the already reduced molecule at different pH values. The reduction of the nitro group has an irreversible peak at approximately -370 mV at pH 3 that corresponds to a four-electron process described in Eq. (1) while at alkaline pH values this peak is split into one redox couple (Eq. (2)) and one irreversible cathodic peak (Eq. (3)). Furthermore, the reduction of the imino group of the hydroxylamine derivative appears at potentials near the solvent discharge as a cathodic irreversible process. We concentrated our attention on the response due to the nitro group. In Fig. 7 at pH 9 and 12 we observe one redox reversible couple due to a one-electron transfer for the nitro radical anion formation (peak I, Eq. (2)). There is also another irreversible peak due to a three-electron reduction process that corresponds to the hydroxylamine derivative formation from the nitro radical anion (peak I′, Eq. (3)). This is in good agreement with the well-known mechanism for the reduction of nitro compounds at alkaline pH [10]. Fig. 8 shows the behavior of the isolated redox couple (RNO_2/RNO_2^-) with the sweep rate. Both the $E_{p,c}$ and current ratio, $I_{p,a}/I_{p,c}$, remain constant with the increase of sweep rate. This indicates that the process is reversible and is not coupled with a chemical reaction [18].

Fig. 9 shows the cyclic voltammogram for compound **E**. In this case the first electron reduction transfer (peak III) corresponds to the formation of the radical anion $\mathbf{E}^{\bullet -}$ from **E**. The most basic site of this radical anion is one of the nitrogens of the azo group and its protonation leads to the hydrazo derivative of **E**, through a classical electronation–protonation mechanism (two electrons, two protons):

$$\mathrm{Ar{-}N{=}N{-}Ar{-}NO_2} + 2\mathrm{e}^- + 2\mathrm{H}^+ \rightarrow \mathrm{Ar{-}NH{-}NH{-}Ar{-}NO_2} \quad (4)$$

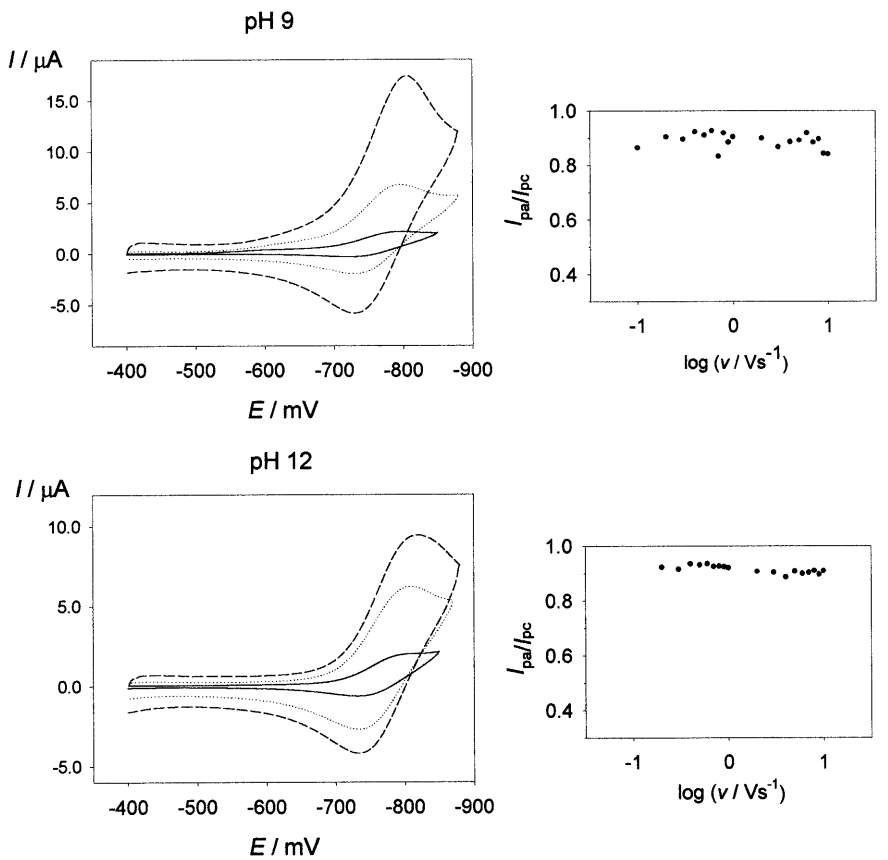

Fig. 8. Cyclic voltammograms of the nitro/nitro radical anion couple of compound **A** in mixed media at different sweep rates and pH values 9 and 12. 0.5 V s^{-1} (—), 1 V s^{-1} (···), 5 V s^{-1} (---). Inserts: the corresponding current ratio versus sweep rate.

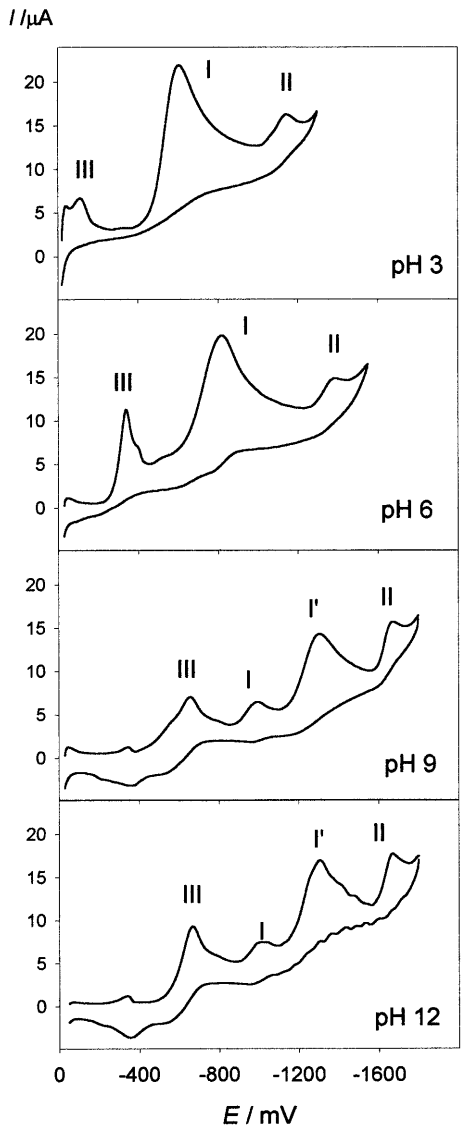

Fig. 9. Cyclic voltammograms of 1 mM of compound **E** in mixed media, DMF + citrate buffer: 60/40 at different pH values. Sweep rate 1 V s^{-1}.

This reduction process produces an irreversible peak (peak III) appearing at pH 3 (-200 mV) and pH 6 (-350 mV). At alkaline pH, this peak became reversible.

In the same figure, peak I corresponds to the nitro reduction of the hydrazo derivative to form the hydrazo–hydroxylamine derivative. This peak shows the typical behavior of nitroaromatic compounds with only one irreversible peak at acidic pH (Eq. (1)) and two peaks at alkaline pH values (Eqs. (2) and (3), peaks I, I′). Peak I corresponds to the nitro/nitro radical anion couple that is not well resolved since it overlaps with the azo group peak and consequently, precise current ratios were not obtained. The anodic peak appearing at about -400 mV at pH values 9 and 12 could be ascribed to the oxidation of the hydrazo–hydroxylamine derivative to form the hydrazo–nitroso derivative.

$$\text{Ar–NH–NH–Ar–NHOH} \rightarrow \text{Ar–NH–NH–Ar–NO} + 2\text{H}^+ + 2\text{e}^- \quad (5)$$

Finally, peak II corresponds to the reduction of the imino group of the hydrazo–hydroxylamine derivative.

The formation of the nitro radical anion in aprotic medium was also studied for all compounds (see Fig. 10). For compound **E**, it was not possible to obtain quantitative information because the signals of the couple interfered with the signal of the azo group. Fig. 10 shows the behavior of the nitro/nitro radical anion couples for compounds **A**–**D**. In all the cases the current ratio, $I_{p,a}/I_{p,c}$, increases towards unity when the sweep rate is increased. Furthermore, the $I_{p,a}/I_{p,c}$ value is concentration dependent which allows us to conclude that the process follows an EC_2 mechanism wherein the first step is the one-electron reduction to produce the nitro radical anion and the second step is a second order chemical reaction. We have employed a previously described procedure [19,20] in order to calculate the second order decay constants.

Table 2 reports the peak potential of the nitro radical anion formation and the second order decay rate constant (k_2). From this table, all **A**–**D** compounds produce the nitro radical anion with the same energy requirements and also there are no significant differences in the decay of the radical anions under these conditions.

In conclusion both electrochemical and spectroscopic evidence permit us to decide about the push–pull effect on the studied liquid crystal molecules. First, spectroscopic evidence clearly shows an enhancement of the push–pull effect in molecule **E** due to the presence of the azo bridge. Secondly, electrochemical evidence using the nitro group as a probe, indicates clearly that electron-donating groups at the end opposite to the nitro group produce an enhancement of the push–pull effect in the molecules.

Acknowledgements

This work was supported by FONDECYT 1000853, DID-Universidad de Chile and Facultad de Ciencias Químicas y Farmacéuticas, Universidad de Chile, Project CEPEDEQ-Facultad.

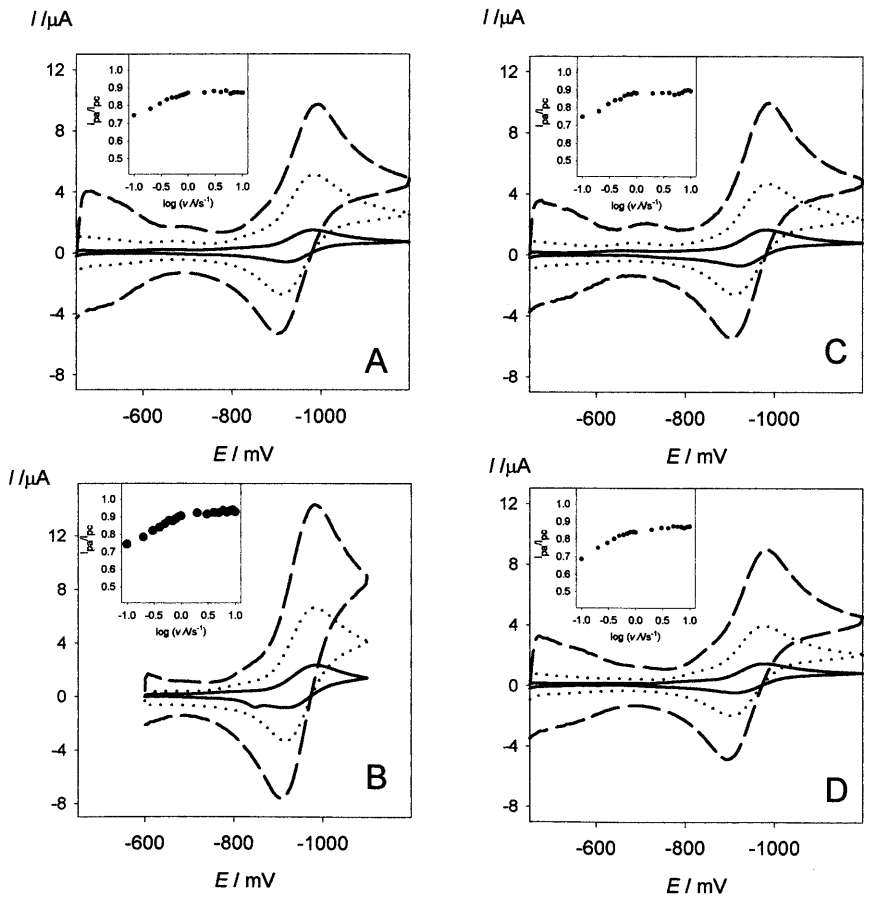

Fig. 10. Cyclic voltammograms showing the nitro/nitro radical anion couple of several nitrostilbene derivatives (**A**–**D**) in DMF at different sweep rates. 0.5 V s^{-1} (—), 1 V s^{-1} (···), 5 V s^{-1} (---). Inserts: the corresponding current ratio versus sweep rate.

Table 2
Cathodic peak potential and the second order decay constant of the nitro radical anion from several nitrostilbene derivatives in aprotic medium

Compound	E_p/mV	$10^3\ k_2$/l mol^{-1} s^{-1}
A	−986	2.8
B	−994	3.6
C	−990	1.9
D	−982	2.1
E	−1050	[a]

[a] Couple poorly resolved.

References

[1] P.N. Prasad, D.J. Williams, Introduction to Nonlinear Optical Effects in Molecules and Polymers, first ed., Wiley, New York, 1991.
[2] J.C. Baumert, R.J. Twieg, G.C. Bjorklund, J.A. Logan, C.W. Dirk, Appl. Phys. Lett. 51 (1987) 1484.
[3] D. Dorsch, B. Rieger, H. Franke, Merck Patent, Ger. Offen. DE 3,819,801, 14 Dic, 1989.
[4] K.D. Singer, W.R. Holland, M.G. Kuzyk, G.L. Wolk, P.A. Cahill, Mol. Cryst. Liq. Cryst. 189 (1990) 123.
[5] M.S. Paley, J.M. Harris, H. Looser, J.C. Baumert, G.C. Bjorklund, D. Jundt, R.J. Twieg, J. Org. Chem. 54 (1989) 3774.
[6] (a) P.D. Maker, R.W. Terhune, M. Nisenoff, C.M. Savage, Phys. Rev. Lett. 8 (1962) 21. (b) J. Jerphagnon, S.K. Kurtz, J. Appl. Phys. 41 (1970) 1667.
[7] T. Hanemann, E.A. Soto Bustamante, T. Weyrauch, W. Haase, Liq. Cryst. 14 (1993) 635.
[8] E.A. Soto Bustamante, W. Haase, Liq. Cryst. 23 (1997) 603.
[9] J.A. Squella, J.C. Sturm, B. Weiss-Lopez, M. Bontá, L.J. Núñez-Vergara, J. Electroanal. Chem. 466 (1999) 90.
[10] H. Lund, in: H. Lund, M. Baizer (Eds.), Organic Electrochemistry, third ed., Dekker, New York, 1990 (Chapter III).
[11] B. Kastening, in: P. Zuman, L. Meites, I.M. Kolthoff (Eds.), Progress in Polarography, vol. 3, Wiley, New York, 1972.
[12] E. Laviron, R. Meunier-Prest, R. Lacasse, J. Electroanal. Chem. 375 (1994) 263.
[13] J.A. Squella, M. Huerta, S. Bollo, H. Pessoa, L.J. Núñez-Vergara, J. Electroanal. Chem. 420 (1997) 63.
[14] A. Cyr, P. Huot, G. Belot, J. Lessard, Electrochim. Acta 35 (1990) 147.
[15] C. Karakus, P. Zuman, J. Electroanal. Chem. 396 (1995) 499.
[16] A.G. Gonzalez, F. Pablos, A. Asuero, Talanta 39 (1992) 91.
[17] A. Asuero, M.A. Herrador, G. Gonzalez, Talanta 40 (1993) 479.
[18] D.K. Gosser, Cyclic Voltammetry Simulation and Analysis of Reaction Mechanism, VCH, New York, 1994 (Chapter 2).
[19] L.J. Núñez-Vergara, F. García, M. Dominguez, J. De la Fuente, J.A. Squella, J. Electroanal. Chem. 381 (1995) 215.
[20] M.L. Olmstead, R.G. Hamilton, R.S. Nicholson, Anal. Chem. 41 (1969) 260.